Variation in Protein Indirect Relaxation Effects in One- and Two-Dimensional Exchange-Transferred Overhauser Experiments

Jie Zheng[†] and Carol Beth Post*

Department of Medicinal Chemistry and Biological Sciences, Purdue University, West Lafayette, Indiana 47907-1333

Received: October 5, 1995; In Final Form: December 7, 1995[⊗]

Exchange-transferred nuclear Overhauser experiments (NOE) probe the three-dimensional conformation of small-molecule ligands bound to macromolecules and have been used to study ligand structural features in a number of ligand−protein complexes. A complete rate matrix analysis, including interactions between the ligand and macromolecule, of a selective saturation, one-dimensional transferred experiment is reported here to supplement previous matrix descriptions for inversion recovery, two-dimensional experiments. Simulation studies allowed a comparison of the magnitude of indirect relaxation effects from pathways involving the protein between these alternative perturbation experiments. The results show that the effect on a ligand−ligand transferred-NOE intensity from protein indirect relaxation pathways varies between a saturation 1D experiment and a recovery 2D experiment. Attenuation by intermolecular indirect relaxation is diminished in the saturation experiment, while intermolecular relaxation effects that increase the direct NOE intensity are somewhat larger in the saturation experiment. These variations between alternative perturbations result from the relatively large NOE magnetization of the protein spins produced by the continuous saturation of a ligand spin and the particular averaging of NMR relaxation rates when the ligand is in molar excess and undergoes fast exchange. The variation observed in the indirect effect from intermolecular pathways in an exchange system does not occur either with intramolecular pathways or in the absence of exchange. The theoretical results suggest that a ratio of NOE intensities from 1D saturation and 2D recovery experiments may be used to indicate regions of close contact between ligand and protein.

Introduction

Exchange-transferred nuclear Overhauser (ET-NOE) experiments probe the three-dimensional conformation of small-molecule ligands bound to macromolecules[1] and have been used to study ligand structural features in a number of ligand−protein complexes (see reviews of refs 2−6). The averaging of NMR quantities by rapid association/dissociation of the ligand allows structural studies related to macromolecules of molecular weight too large to be observed directly by NMR.[7] In an ET-NOE experiment, the ligand and macromolecule are present in solution with the ligand in molar excess. Information on interproton distances between ligand nuclei is obtained from the NOE magnetization measured from the relatively narrow NMR resonances of the ligand. The line widths of these resonances are narrowed due to exchange averaging that is dominated by the free state. However, the averaged NOE magnetization is dominated by cross relaxation in the bound state.

As with conventional NOE interactions in the absence of exchange, ET-NOE magnetization is measured by perturbations from equilibrium by either a continuous saturation method or a transient recovery method.[8,9] In the former case, the approach to a new steady-state level of magnetization of the system, driven by selective saturation of a single spin, is followed using one-dimensional spectroscopy. Thus, this experiment reflects the response to continuous irradiation, and sometimes is described as "truncated-driven" NOE. In the case of the transient recovery, either one or all spin magnetization levels are inverted and the rate at which equilibrium is recovered is followed. Recovery experiments may be carried out by either one-dimensional or two-dimensional spectroscopy, with the most common being the two-dimensional, nonselective inversion recovery experiment (ET-NOESY).

Of primary interest in protein−ligand ET-NOE structural studies is the estimation of the distance between two ligand protons. Estimates are determined with varying degrees of accuracy. Under some circumstances, which include the limit of fast exchange, the distance can be determined from the initial slope of the time dependence of the ET-NOE.[10,11] However, it is common that more qualitative estimates are obtained at longer times of the NOE buildup. Several factors, such as indirect effects from multiple-spin relaxation, the exchange rate, and internal motions, affect the measured ET-NOE intensity at these longer mixing times and can lead to errors in distance estimates. A recent and thorough review describing these factors has appeared.[11] The study presented here expands upon current understanding of the influence of indirect relaxation pathways from protons on the macromolecule,[10,12−14] by examining how the size of the macromolecular indirect effects varies in driven compared to transient recovery ET-NOE experiments due to the combined factors of exchange and alternative perturbations of the equilibrium magnetization. Recent experimental results have shown the importance of considering such indirect pathways involving the protein in a protein−ligand complex.[15,16]

We compare the multiproton indirect effects, or spin diffusion, encountered in a one-dimensional selective saturation ET-NOE experiment with that in a two-dimensional inversion recovery ET-NOESY experiment. Indirect effects are changes in the NOE intensity that arise from relaxation pathways other than those of direct cross relaxation between the two protons defining the NOE (Scheme 1A). A matrix approach is described for

* Corresponding author (E-mail: cbp@cc.purdue.edu).
[†] Current address: Laboratories of the Rockefeller University, New York, NY 10021 (E-mail: zhengj@mriris.rockefeller.edu).
[⊗] Abstract published in *Advance ACS Abstracts,* January 15, 1996.

0022-3654/96/20100-2675$12.00/0

SCHEME 1

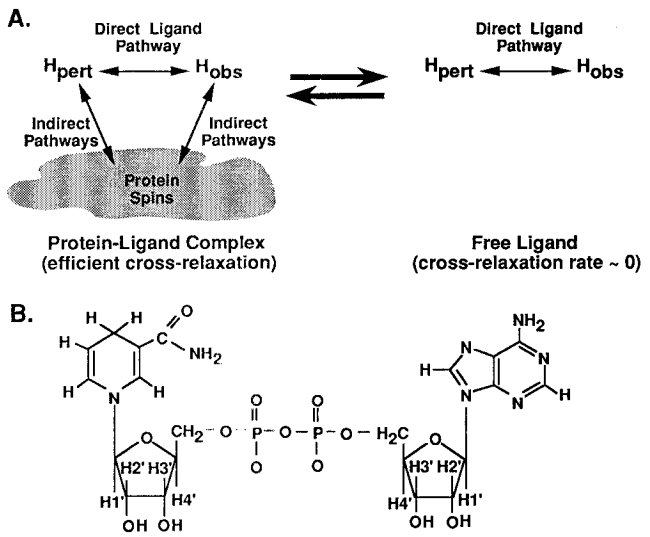

analysis of one-dimensional, selective-saturation-transferred NOE experiments that takes into account these multiple pairwise interactions, including intermolecular pathways between the ligand and macromolecule. To facilitate matrix diagonalization, we use a symmetrization procedure that depends on exchange being fast relative to cross-relaxation, first described by Landy and Rao.[17] Others have subsequently employed a matrix analysis of two-dimensional experiments on exchange systems (refs 4,6 and references therein). This report is the extension of our previous work[12] to such a matrix analysis of selective saturation ET-NOE and a comparison of protein indirect effects with the alternative perturbation conditions.

By using simulations of the protein complex lactate dehydrogenase·nicotinamide adenine dinucleotide (LDH·NADH), we show that the combination of alternative perturbation and ligand exchange produces different amounts of protein-modulated indirect effects. For certain NOE interactions, where the direct NOE intensity is attenuated by relaxation with the protein, these effects are less pronounced with saturating conditions. However, for other interactions, where the intensity is enhanced by the protein spins, indirect effects are significant with both saturating and recovery conditions. The results suggest that variations between one-dimensional saturation and two-dimensional recovery experiments may be used to indicate regions of close contact between the ligand and macromolecule.

Theory

Selective Saturation 1D ET-NOE. For a system of two dipolar coupled spins, *i* and *j*, irradiation of *j* causes a change in the resonance intensity of *i*. The nuclear Overhauser effect on the intensity of spin *i* is defined as

$$\eta_i(t) = \frac{I_{iz} - I_{i0}}{I_{i0}} \tag{1}$$

where I_{iz} is the *z* magnetization of spin *i*, and I_{i0} is the equilibrium value of I_{iz}. In an *n*-spin system, the time-dependent magnetization response to selective saturation of spin *j* can be described by a set of $(n-1)$ equations. Using matrix notation, these equations are written as[18,19]

$$\frac{\mathrm{d}[\eta]}{\mathrm{d}t} = -\mathbf{\Gamma}'[\eta] + [\sigma] \tag{2}$$

where $[\eta]$ is a column array of $(n-1)$ NOE intensities excluding *j*, *t* is the mixing time, and $[\sigma]$ is a column array of the cross-relaxation rates, σ_{ij}, between spin *j* and all other $(n-1)$ spins. The relaxation rate matrix $\mathbf{\Gamma}'$ excludes spin *j* by deleting the *j*th column and *j*th row from the full relaxation matrix $\mathbf{\Gamma}$ of the *n*-spin system defined as

$$\mathbf{\Gamma} = \begin{bmatrix} \varrho_1 & \sigma_{12} & \sigma_{13} & \cdots \\ \sigma_{21} & \varrho_2 & \sigma_{23} & \cdots \\ \sigma_{31} & \sigma_{32} & \varrho_3 & \cdots \\ \vdots & \vdots & \vdots & \vdots \end{bmatrix}$$

The diagonal elements, ρi, are the self-relaxation rates for each spin *i*. Both σ_{ij} and ρi, are functions of the inverse sixth power of the distance between a proton pair.

A solution to the inhomogeneous eq 2 is[20]

$$[\eta] = \int_0^t \mathrm{e}^{-\mathbf{\Gamma}'(t-s)}[\sigma]\,\mathrm{d}s \tag{3}$$

Integration of this equation and substitution with the eigenvalues and eigenvector of $\mathbf{\Gamma}'$ gives

$$[\eta] = \mathbf{K} \times \begin{bmatrix} \ddots & & 0 \\ & \frac{1}{l_i}(1 - \mathrm{e}^{-l_i t}) & \\ 0 & & \ddots \end{bmatrix} \times \mathbf{K}^{\mathrm{T}} \times [\sigma] \tag{4}$$

Matrix **K** contains the eigenvectors of Γ', and l_i in the diagonal elements are the eigenvalues of Γ'. The evaluation of the Overhauser enhancements is therefore reduced to the eigenvalue problem of determining **K** and l_i.

In an exchange-transferred system, the ligand, L, and protein, P, have two states: bound and free.

$$\mathrm{P} + \mathrm{L} \underset{k_{-1}}{\overset{k_1}{\rightleftharpoons}} \mathrm{PL}$$

The full rate matrix for this system, $\mathbf{\Gamma}_{\mathrm{ex}}$, includes the exchange terms as well as magnetic relaxation terms. In particular, $\mathbf{\Gamma}_{\mathrm{ex}}$ comprises cross-relaxation rates for P, L, and the complex PL where both inter- and intramolecular pairwise terms are present. The cross-relaxation rates are large for P and PL, whereas these rates are near zero for free L since its rotational correlation time is near the magnetic Larmor frequency. As such, $\mathbf{\Gamma}_{\mathrm{ex}}$ is written as

$$\mathbf{\Gamma}_{\mathrm{ex}} = \begin{bmatrix} \mathbf{\Gamma}_{\mathrm{l}}^{\mathrm{b}} + k_{-1}\mathbf{1} & -k_1[\mathrm{P}]\mathbf{1} & \mathbf{\Gamma}_{\mathrm{lp}}^{\mathrm{b}} & \mathbf{0} \\ -k_{-1}\mathbf{1} & \mathbf{\Gamma}_{\mathrm{l}}^{\mathrm{f}} + k_1[\mathrm{P}]\mathbf{1} & \mathbf{0} & \mathbf{0} \\ \mathbf{\Gamma}_{\mathrm{pl}}^{\mathrm{b}} & \mathbf{0} & \mathbf{\Gamma}_{\mathrm{p}}^{\mathrm{b}} + k_{-1}\mathbf{1} & -k_1[\mathrm{L}]\mathbf{1} \\ \mathbf{0} & \mathbf{0} & -k_{-1}\mathbf{1} & \mathbf{\Gamma}_{\mathrm{p}}^{\mathrm{f}} + k_1[\mathrm{L}]\mathbf{1} \end{bmatrix}$$

The superscripts b and f refer to bound and free species, respectively, the subscripts p and l refer to an intramolecular rate in protein and ligand, respectively, and the subscripts pl and lp refer to an intermolecular rate in the complex. **1** is an identity matrix, and **0** is a null matrix of appropriate dimensions. [P] and [L] are the concentration of protein and ligand in solution. At the fast exchange limit k_1, $k_{-1} \gg \rho$, σ, and by assuming the exchange is fast relative to chemical shift differences so that free and bound states of a proton appear at

a single resonance, the rate matrix can be simplified as follows:[12−14]

$$\mathbf{\Gamma}_{ex} = \begin{bmatrix} \dfrac{[PL]\mathbf{\Gamma}_l^b + [L]\mathbf{\Gamma}_l^f}{[PL]+[L]} & \dfrac{[PL]\mathbf{\Gamma}_{lp}^b}{\sqrt{([P]+[PL])([L]+[PL])}} \\ \dfrac{[PL]\mathbf{\Gamma}_{pl}^b}{\sqrt{([P]+[PL])([L]+[PL])}} & \dfrac{[PL]\mathbf{\Gamma}_p^b + [P]\mathbf{\Gamma}_p^f}{[PL]+[P]} \end{bmatrix} \quad (5)$$

For selective saturation of ligand resonance *j*, the NOE of the observed spins builds to a steady-state level at long mixing times, and the matrix $\mathbf{\Gamma}'_{ex}$ differs from the full matrix $\mathbf{\Gamma}_{ex}$ (eq 5) by deleting the appropriate column and row for the saturated proton, as described above. Equation 2 in the presence of fast exchange becomes

$$\frac{d}{dt}\begin{bmatrix} \eta_l^b + \eta_l^f \\ \sqrt{\dfrac{[L]+[PL]}{[P]+[PL]}}(\eta_p^b + \eta_p^f) \end{bmatrix} = -\mathbf{\Gamma}'_{ex}\begin{bmatrix} \eta_l^b + \eta_l^f \\ \sqrt{\dfrac{[L]+[PL]}{[P]+[PL]}}(\eta_p^b + \eta_p^f) \end{bmatrix} + \begin{bmatrix} \sigma_{ll}^{ex} \\ \sigma_{pl}^{ex} \end{bmatrix} \quad (6)$$

where the averaged cross-relaxation rate between the irradiated ligand spin *j* and a second ligand spin *i*

$$(\sigma_{ll}^{ex})_{ij} = \frac{[PL]\sigma_{ij}^b + [L]\sigma_{ij}^f}{[PL]+[L]} \quad (7a)$$

is and that between spin *j* and a protein spin *i* is

$$(\sigma_{pl}^{ex})_{ij} = \frac{[PL]\sigma_{ij}^b}{\sqrt{([P]+[PL])([L]+[PL])}} \quad (7b)$$

As in eq 2,

$$\begin{bmatrix} \eta_l^b + \eta_l^f \\ \sqrt{\dfrac{[L]+[PL]}{[P]+[PL]}}(\eta_p^b + \eta_p^f) \end{bmatrix}$$

is a column array of ET-NOEs that excludes the intensity for the irridiated spin *j*, and

$$\begin{bmatrix} \sigma_{ll}^{ex} \\ \sigma_{pl}^{ex} \end{bmatrix}$$

is a column array of cross-relaxation rates between the saturated proton *j* and all other protons *i* of ligand or protein.

The solution to eq 6 for selective saturation in the presence of chemical exchange is expressed in terms of the eigenvectors and eigenvalues of $\mathbf{\Gamma}'_{ex}$, similar to eq 4

$$\begin{bmatrix} \eta_l^b + \eta_l^f \\ \sqrt{\dfrac{[L]+[PL]}{[P]+[PL]}}(\eta_p^b + \eta_p^f) \end{bmatrix} = \mathbf{K}_{ex} \times \begin{bmatrix} \ddots & & 0 \\ & \dfrac{1}{(l_{ex})_i}(1 - e^{-(l_{ex})_i t}) & \\ 0 & & \ddots \end{bmatrix} \times \mathbf{K}_{ex}^{T} \times \begin{bmatrix} \sigma_{ll}^{ex} \\ \sigma_{pl}^{ex} \end{bmatrix} \quad (8)$$

Because $\mathbf{\Gamma}'_{ex}$ is a symmetrical matrix, standard diagonalization methods can be used to calculate the eigenvalues $(l_{ex})_i$ and eigenvectors $\mathbf{K}_{ex}$.

2D ET-NOESY. A complete description, including intermolecular cross relaxation, of the 2D ET-NOESY in the fast exchange limit with respect to cross-relaxation rates has been reported.[10,12−14] Under the condition $k_1[P] + k_{-1} \gg \rho, \sigma$, the time-dependence of the peak volumes for rapidly averaged free and bound proton resonances is given by

$$\frac{d}{dt_m}\begin{bmatrix} \sqrt{[P]+[PL]}(\mathbf{V}_l^b + \mathbf{V}_l^f) \\ \sqrt{[L]+[PL]}(\mathbf{V}_p^b + \mathbf{V}_p^f) \end{bmatrix} = -\mathbf{\Gamma}_{ex}\begin{bmatrix} \sqrt{[P]+[PL]}(\mathbf{V}_l^b + \mathbf{V}_l^f) \\ \sqrt{[L]+[PL]}(\mathbf{V}_p^b + \mathbf{V}_p^f) \end{bmatrix} \quad (9)$$

The elements of matrices **V** are the peak volumes in the ET-NOESY spectrum. The solution to eq 9 is straightforward[12] and requires diagonalization of the symmetrical matrix $\mathbf{\Gamma}_{ex.}$

Simulation Method

We examine by computer simulations the time-dependent ET-NOE intensities of NADH (Scheme 1B) in the presence of dogfish LDH (M_r = 140 000) produced by the alternative perturbation conditions of selective saturation or inversion recovery. The LDH·NADH system is similar in molecular weight and correlation time to protein complexes on which many ET-NOE experiments are performed. Moreover, this system demonstrates a range of indirect magnetization effects that vary in size due to different spatial arrangements of protein protons near a ligand−ligand NOE pair. In the LDH·NADH complex, nicotinamide is buried within the protein, while adenine is bound on the surface of the protein.[21] Therefore, there are more protein protons in close proximity to the nicotinamide-ribose moiety than the adenine-ribose moiety. Hydrogen atom coordinates were determined by geometry from the heavy atoms in a crystallographic structure of LDH·NADH using the program CHARMM. Coordinates were obtained from the X-ray crystallographic structure for the ternary complex (J. Griffith and M. Rossmann, Brookhaven Protein Data entry 1LDM) with the substrate analogue, oxamate, deleted. The energy of the LDH·NADH structure was minimized and the optimized structure was used in the NMR simulation studies. The correlation time for LDH and the LDH·NADH complex was 60 ns, and for free NADH, 0.4 ns. The total concentrations of NADH and tetrameric LDH were 5 and 0.125 mM, respectively, and the binding equilibrium constant, K_d, equals 3.6 μM,[21] giving approximately 0.125 mM for the final LDH·NADH complex concentration and 0.5 mM bound NADH. A 500 MHz magnetic field and fast exchange with respect to cross relaxation are assumed for all calculations.

Results

Four ligand−ligand ET-NOE interactions were examined: H1′−H4′ and H2′−H3′ in the ribose of the adenine or nicotine base. The ring puckering is nearly identical for the two ribose rings, so that the interproton distances for similar proton pairs are nearly equal. The distances for H1′−H4′ and H2′−H3′ are 2.87 and 2.42 Å in the adenine moiety and 2.76 and 2.46 Å in the nicotinamide moiety, respectively. Figure 1 shows the time-development of the ET-NOE intensity for the four ligand pairs. The ET-NOE for proton pairs with similar distances appear in columns a and b for nicotinamide $H1'_N-H4'_N$ and adenine $H1'_A-H4'_A$ and in columns c and d for $H2'_N-H3'_N$ and $H2'_A-H3'_A$, respectively. The time-dependence of the ET-NOE is

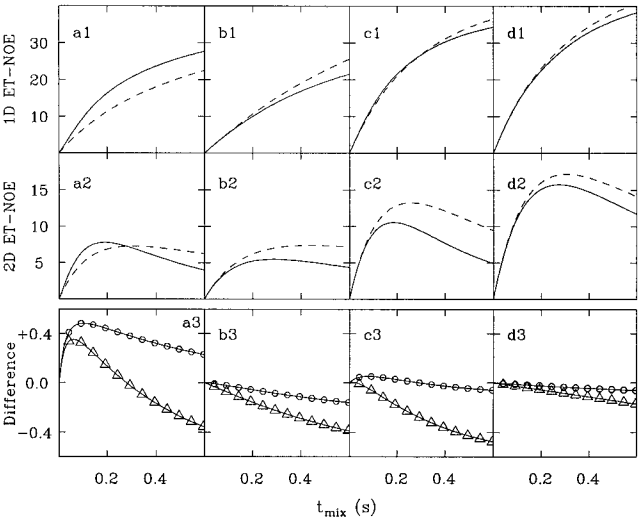

Figure 1. Simulated time-dependence of ET-NOE intensities for alternative perturbation conditions of the ligand proton pairs: (a) $H1'_N-H4'_N$; (b) $H1'_A-H4'_A$; (c) $H2'_N-H3'_N$; and (d) $H2'_A-H3'_A$. Top panels: selective saturation, 1D ET-NOE time-development curves (eq 8). Middle panels: time-development of inversion recovery 2D ET-NOESY cross-peak intensities (solution to eq 9). Two sets of simulations are shown: (solid curves) NADH and LDH protons within 10 Å of the binding site are included in the rate matrix to best approximate observed intensities; (dashed curves) only the protons on NADH are included in the rate matrix, as if LDH were fully deuterated. Bottom panels: the relative difference in the ET-NOE intensity with and without protein protons in the relaxation matrix divided by that with the protein protons ((solid−dashed)/solid) to show the intermolecular indirect effect in the selective saturation 1D experiment (circles) and the transient ET-NOESY (triangles). No contribution to relaxation from the protein would give a zero vertical value. The simulations used the coordinates from the X-ray crystallographic structure of NADH·LDH; a correlation time equal to 60 ns for LDH·NADH and 0.4 ns for free NADH, 500 MHz field strength, 5 mM [NADH], 0.125 mM [LDH], and 3.6 μM K_D, giving approximately 0.5 mM LDH·NADH subunits.

shown in the top row for selective saturation calculated from eq 8 and in the middle row for the inversion recovery in a 2D ET-NOESY experiment calculated from the solution to eq 9.

Two sets of simulations were performed: the first set of calculations (solid lines) includes protons of LDH and NADH in the rate matrix and best approximates observed intensities, whereas the second set (dashed curves) includes NADH protons only, as if the protein were fully deuterated. Thus, we use as a reference the isolated ligand undergoing exchange and therefore subject to the population-weighted average of relaxation rates, such that the dashed curves would be the results calculated by a multiple-spin approach without information on the macromolecule. Referring to Scheme 1A, this reference is the exchange system without the pool of indirect spins. The contribution to the ligand−ligand ET-NOE intensity from indirect effects caused by relaxation with protons from the protein is the difference between the NOE intensity calculated with and without the protein protons in the relaxation matrix. This indirect contribution is plotted as a percentage of the full intensity (solid curves) in the bottom row of Figure 1 for the selective saturation experiment (circles) and the recovery 2D ET-NOESY experiment (triangles). In a case where the intermolecular relaxation pathways have negligible effect, the solid and dashed curves in the top and middle rows would be similar, and the relative difference shown in the bottom row would be near to zero.

The well-known effect from indirect relaxation[19,22−24] is evident in Figure 1. The dashed curves of columns a and b are similar, as expected for similar interproton distances. However, the solid curves in columns a and b are dissimilar, showing the presence of intermolecular indirect effects. Comparing the recovery NOE time courses shown in c2 and d2, both solid and dashed curves differ, even though these two spin pairs are nearly the same distance apart. Thus, both inter- and intramolecular indirect effects are present.

Discussion

The deviation between the ET-NOE intensities calculated for a protiated protein (solid curves) and a deuterated one (dashed curves) indicates the indirect effect from protein-modulated relaxation. A notable feature of Figure 1 is the larger discrepancy between the solid and dashed curves in panels b2, c2, and d2 compared to that in panels b1, c1, and d1. That is, at mixing times greater than 100 ms, the attenuation from protein indirect relaxation pathways is more significant in a 2D recovery experiment than in a continuous saturation experiment. Indeed, in the case of selective saturation (Figure 1, b1, c1, and d1), the attenuation by indirect contributions from the protein is negligible. It is known from previous work[12] that 2D ET-NOESY ligand cross peaks can be attenuated by relaxation with the protein. However, what has not been previously recognized is that *in the case of selective saturation the intensity loss by intermolecular indirect effects is small*, even when a substantial loss occurs in a 2D recovery experiment. This variation between the alternative perturbation experiments is more pronounced for $H2'_N-H3'_N$ (Figure 1, c1 vs c2) than $H2'_A-H3'_A$ (Figure 1, d vs d2) or $H1'_A-H4'_A$ (Figure 1, b1 vs b2) because of a larger number of LDH protons in close proximity to both $H2'_N$ and $H3'_N$. The number of LDH protons within 5 Å of both protons of the direct NOE pair is seven, three, and four for $H2'_N-H3'_N$ (panels c), $H2'_A-H3'_A$ (panels d), and $H1'_A-H4'_A$ (panels b), respectively.

Unlike the NOE attenuation in Figure 1, panels b, c, and d, the NOE intensity at short t_{mix} for $H1'_N-H4'_N$, shown in panel a, is enhanced by indirect interactions. These indirect effects are significant given either perturbation condition. The distance from either $H1'_N$ or $H4'_N$ to the LDH proton, Ser137 Hα, is shorter than the separation between $H1'_N$ and $H4'_N$. Thus, the NOE magnetization developed by 137 Hα from perturbations of either $H1'_N$ or $H4'_N$ is greater than the direct NOE magnetization so that indirect interactions increase the observed NOE.

The variation in the protein-modulated indirect effects between the 1D selective saturation experiment and the 2D inversion recovery experiment (circles vs triangles in Figure 1, row 3) arises from both the exchange averaging of magnetic relaxation and that the indirect pathways are from the protein, and not the ligand. That is, there is no significant variation in indirect contributions using these alternative perturbation methods either in the absence of exchange or when spin diffusion originates within the ligand in an exchange system.

To demonstrate that the variation occurs for intermolecular but not intramolecular spin diffusion, we invoke a hypothetical LDH·NADH exchange system in which the protein protons near one of the ligand protons for a direct NOE interaction are treated as ligand protons. Thus, LDH protons within 5 Å of $H2'_N$ from NADH were labeled as ligand spins in the hypothetical system, instead of protein spins as in the actual system. These indirect spins have the same spatial arrangement, but populations of free and bound states corresponding to NADH, as if part of the pool of indirect spins in Scheme 1A, also appear on the right-hand side.

The time-development of the $H2'_N-H3'_N$ transferred NOE is shown in Figure 2A for the 1D selective saturation experiment

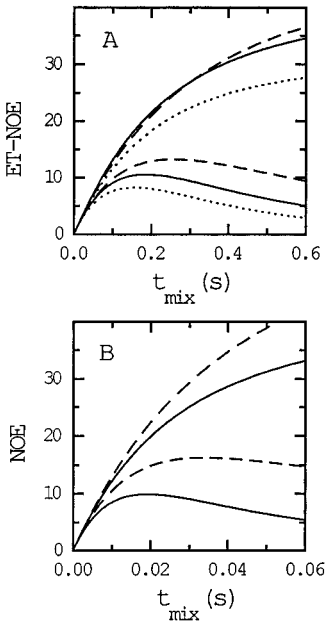

Figure 2. Time-development curves of the transferred NOE with alternative perturbations for $H2'_N-H3'_N$. The upper curves are the result of selective saturation 1D ET-NOE, and the lower curves are from inversion recovery observed with 2D ET-NOESY. Parameters are as in Figure 1. (A) Disparate behavior of intermolecular and intramolecular indirect relaxation in an exchange system. The dotted curves (intramolecular spin diffusion) are the buildup curves in a hypothetical LDH·NADH complex in which 10 spins of LDH near $H2'_N$ are treated as ligand spins. See text for detail. The solid (intermolecular spin diffusion) and dashed (reference) curves are as in Figure 1, c1 and c2. The deviation between dotted and dashed curves, the intramolecular indirect effects, is similar with alternative perturbations, while that between the solid and dashed curves, the intermolecular indirect effect, is not. (B) Effect of indirect relaxation in the absence of exchange, i.e., the time-development for the LDH·NADH complex without a molar excess of NADH. The solid curves calculated for protiated LDH include indirect effects. The dashed curves for deuterated LDH serve as the reference without protein indirect effects. The scale of t_{mix} reflects the ratio of the free ligand to bound ligand concentrations.

(upper curves) and 2D recovery experiment (lower curves). The dotted curves in Figure 2A are the time-development of the hypothetical system in which 10 spins of LDH near $H2'_N$ were treated as ligand spins. The solid and dashed curves are as in Figure 1, c1 and c2, and correspond to the actual systems of LDH·NADH and the NADH reference, respectively. Deviations from the dashed curve (NADH reference) occurs by indirect relaxation, with the 10 protons in question corresponding to either intramolecular interactions within the hypothetical ligand (dashed vs dotted) or the analogous intermolecular interactions of the actual LDH·NADH complex (dashed vs solid). For intramolecular spin diffusion, the attenuation shown in Figure 2A is nearly the same with the alternative perturbation methods, in contrast to the disparate attenuation for intermolecular spin diffusion.

That the indirect contributions attenuate the direct NOE intensity equally with saturation and recovery experiments in the absence of exchange is also readily demonstrated. Figure 2B shows the time-development of the two experiments for the conventional NOE between $H2'_N-H3'_N$ in the complex, without exchange. As above, the solid curves were calculated including protons from the full NADH·LDH complex, and the dashed curves were calculated with NADH protons only, as if LDH were fully deuterated. The effect from spin diffusion is similar in the saturation experiment and the recovery experiment. (Whether the indirect interactions are intermolecular or intramolecular is irrelevant in the absence of exchange.)

The variation between alternative perturbation experiments in the effect from spin diffusion is a result of the exchange process averaging differently the NMR relaxation rates for the indirect and direct interactions. If the pool of indirect spins is part of the ligand (such that it appears on both sides of the arrows in Scheme 1A), then the indirect interactions and the direct $H_{pert}-H_{obs}$ interaction are governed by the same population-weighted averaging, in which the free ligand is the major fraction. However, if the pool is part of the protein, the indirect spins are governed by the rates of only the complex (since the protein is saturated with ligand), while the direct $H_{pert}-H_{obs}$ spins experience free and bound states. When the indirect interactions come from the protein spins, the cross-relaxation rates are averaged as the off-diagonal elements in eq 5, while the equilibrium average for the direct ligand−ligand interaction is the expression shown on the diagonal in eq 5. For the conditions of large molar excess in ligand, the indirect, off-diagonal rates are larger by approximately $[L]^{1/2}$.

The basis for the smaller attenuation in 1D saturation experiments from intermolecular indirect effects, but not intramolecular ones, comes from a more effective cross relaxation of the continuously irradiated H_{pert} with protein spins compared with the ligand spins. The continuous irradiation of H_{pert} produces a larger indirect NOE magnetization for protein spins because the protein spins do not experience the free-state relaxation conditions where cross-relaxation rates are near zero. (The difference due to exchange averaging for cross relaxation of H_{pert} with the protein spins compared to that with the ligand spins is seen by comparing eqs 7b and 7a and is the same as that discussed above.) Because the NOE intensity of the pool of protein indirect spins is relatively enhanced, the attenuation of the direct NOE intensity is smaller.

This basis for less attenuation by indirect effects in a saturation experiment is also the basis for larger enhancements by indirect effects with this type of perturbation, as shown in Figure 1, panel a. The continuous irradiation combined with exchange averaging promotes the contribution of the indirect protein spin, 137 Hα, to increase the direct NOE intensity since the magnetization of 137 Hα by H_{pert} is efficient.

Conclusions

In summary, we have shown using a theoretical matrix analysis of NMR relaxation that the effect on a ligand−ligand ET-NOE intensity from indirect relaxation with protein protons varies between a saturation 1D experiment and a recovery 2D experiment. In the case where indirect relaxation attenuates the direct NOE intensity, the effect is smaller (Figure 1, b2-d1 vs b2-d2) in a 1D saturation experiment. The continuous irradiation of the ligand proton H_{pert} leads to a relatively large NOE magnetization of protein indirect spins and therefore less "drain" on the direct NOE magnetization by protein indirect pathways. The smaller indirect effect does not occur either from intramolecular pathways (Figure 2) or in the absence of exchange. This relative enhancement by cross relaxation between H_{pert} and protein spins is due to the particular averaging of NMR relaxation rates when the ligand is in molar excess and undergoes fast exchange and the protein is saturated with ligand. For the case where a ligand−ligand ET-NOE intensity is increased as a result of the indirect protein pathways, the relatively large indirect NOE intensity produced from exchange averaging and continuous irradiation leads to a greater increase (Figure 1, a1 vs a2).

The variation in protein-modulated indirect effects between alternative perturbation experiments reported here is significant at mixing times greater than 100 ms for a 140 kDa protein and

ligand/binding-site molar ratio of ~10. There is no discernible variation between 1D saturation ET-NOE experiments and 2D recovery experiments at mixing times less than 30 ms. (The initial slopes, albeit for extremely short mixing times, are equal to the equilibrium-averaged direct cross-relaxation rate in all instances, as expected for the limiting condition $t \rightarrow 0$ and fast exchange.[9,25]) However, it should be noted that current structural studies on exchange complexes, in order to obtain reasonable signal/noise, use ET-NOESY intensities measured at mixing times greater than that which satisfies initial conditions.[26−32] Qualitative estimates of interproton distances are obtained from intensities measured at 150−250 ms, where protein-mediated effects can be significant and the discrepancies noted here between 2D recovery and selective saturation would exist. For example, the NOE values at 200 ms of the solid curve in Figure 1, c2 and d2, differ substantially, yet the NOE pairs have nearly equal distances of 2.42 and 2.46 Å, respectively. In contrast, the 1D saturation experiments in Figure 1, c1 and d1, have very similar intensities, more consistent with the interproton distances. Furthermore, in cases where the three-dimensional structure of a ligand molecule determined from ET-NOE intensities is to be verified by a rate matrix analysis that includes only the ligand and not the protein interactions, verification would be most useful for selective saturation time-dependence. Thus, such an analysis would produce the dashed lines in Figure 1, and except for panel a, where the protein-modulated effect enhances the intensity, these curves are more similar to the observed solid curves in the top row than the middle row. Experimental results to demonstrate the behavior described here based on theoretical considerations are of interest and would complement other means for detecting indirect relaxation.[15,16] But, we note that obtaining selectivity in 1D saturation experiments can present a practical problem with large systems such as proteins,[19] as well as the existence of other technical difficulties.[33] Even though the ability to selectively perturb spins can prevent the study of a large number of ligand−ligand NOE interactions by selective 1D experiments, it is nevertheless worthy of consideration for cases where such measurements are feasible.

The variation in the magnitude of the protein indirect effects with alternative perturbation conditions could be exploited to detect regions of the ligand that are in close contact with the protein. Contact regions create buried protein surface in the complex and are likely to have relatively more protein protons in proximity to ligand protons and therefore significant variation in indirect cross relaxation between selective saturation and 2D recovery experiments. The selective saturation intensity at 200 ms (Figure 1, top row) may be compared with the 2D recovery intensity for the same interaction (middle row). The ratio of these intensities is larger for panels a, b, and c (ratio $\geq$ 2.0) than for panel d (ratio ~ 1.5). The three NOE pairs for panels a, b, and c have 22−27 LDH protons within 5.0 Å of either H_{pert} or H_{obs}, while $H2'_A-H3'_A$ in panel d has only six such LDH protons. The larger ratio reflects more effective intermolecular relaxation in the 2D recovery experiment due to a larger number of protein protons near the ligand protons. In the LDH·NADH complex, the nicotinamide moiety is buried and inaccessible to solvent, while the adenine moiety is partially solvent-exposed, with H2′ and H3′ accessible to solvent molecules. On the basis of the current study on the LDH·NADH complex, a ratio of appropriately scaled ET-NOE intensities from a selective saturation and a recovery experiment greater than 2 would indicate a region of the ligand that is well surrounded by protein atoms. The exact value of the ratio would vary with the protein correlation time. Furthermore, we note that a small ratio would not rule out the possibility of close contact since compensating factors (enhancement by an intervening protein spin plus attenuation) could occur, depending on the exact structure.

Acknowledgment. This work was supported in part by a research grant from Public Health Service (GM39478 to C.B.P.) and a grant to the Structure Group, Purdue University, from the Lucille P. Markey Charitable Trust (Michael G. Rossmann, Principal Investigator). Computations were performed on an IBM RS/6000 with the program GUSS, developed in part under an IBM Developer's agreement (to C.B.P.).

References and Notes

(1) Balaram, P.; Bothner-By, A. A.; Breslow, E. *J. Am. Chem. Soc.* **1972**, *94*, 4017-4018.
(2) Rosevear, P. R.; Mildvan, A. S. In *Methods In Enzymology*; Oppenheimer, N. J., James, T. L., Eds.; Academic Press: San Diego, 1989; Vol. 177, pp 333-358.
(3) Anglister, J.; Naider, F. In *Methods In Enzymology*; Langone, J. J., Ed.; Academic Press: San Diego, 1991; Vol. 203, pp 228-241.
(4) Campbell, A. P.; Sykes, B. D. *Annu. Rev. Biophys. Biomol. Struct.* **1993**, *22*, 99−122.
(5) Sykes, B. D. *Curr. Opin. Biotechnol.* **1993**, *4*, 392−396.
(6) Ni, F. *Prog. NMR Spectrosc.* **1994**, *26*, 517−606.
(7) Clore, G. M.; Gronenborn, A. M. *J. Magn. Reson.* **1982**, *48*, 402−417.
(8) Neuhaus, D.; Williamson, M. P. *The Nuclear Overhauser Effect*; VCH Publishers, Inc.: New York, 1989.
(9) Campbell, A. P.; Sykes, B. D. *J. Magn. Reson.* **1991**, *93*, 77−92.
(10) London, R. E.; Perlman, M. E.; Davis, D. G. *J. Magn. Reson.* **1992**, *97*, 79-98.
(11) Ni, F. *J. Magn. Reson.* **1992**, *96*, 651-656.
(12) Zheng, J.; Post, C. B. *J. Magn. Reson. B* **1993**, *101*, 262-270.
(13) Ni, F.; Zhu, Y. *J. Mag. Reson.* **1994**, *103*, 180−184.
(14) Jackson, P. L.; Moseley, H. N. B.; Krishna, N. R. *J. Magn. Reson.* **1995**, *107*, 289−292.
(15) Perlman, M. E.; Davis, D. G.; Koszalka, G. W.; Tuttle, J. V.; London, R. E. *Biochemistry* **1994**, *33*, 7547−7559.
(16) Arepalli, S. R.; Glaudemans, C. P. J.; Daves, G. D., Jr.; Kovac, P.; Bax, A. *J. Magn. Reson.* **1995**, *106*, 195−198.
(17) Landy, S. B.; Rao, B. D. N. *J. Magn. Reson.* **1989**, *81*, 371−377.
(18) Krishna, N. R.; Agresti, D. B.; Glickson, J. D. *Biophys. J.* **1978**, *24*, 791−814.
(19) Dobson, C. M.; Olejniczak, E. T.; Poulsen, F. M.; Ratcliffe, R. G. *J. Magn. Reson.* **1982**, *48*, 97-110.
(20) Braun, M. *Differential Equations and Their Applications, Short Version*; Springer-Verlag, New York, 1975; pp 268.
(21) Holbrook, J. J.; Liljas, A.; Steindel, S. J.; Rossmann, M. G. In *The Enzymes*, 3rd ed.; Boyer, P. D., Ed.; Academic Press: New York, 1975; Vol. XI, pp 191−294.
(22) Keepers, J. W.; James, T. L. *J. Magn. Reson.* **1984**, *57*, 404−426.
(23) Olejniczak, E. T.; Gampe, R. T., Jr.; Fesik, S. W. *J. Magn. Reson.* **1986**, *67*, 28−41.
(24) Post, C. B.; Meadows, R. P.; Gorenstein, D. G. *J. Am. Chem. Soc.* **1990**, *112*, 6796−6803.
(25) Clore, G. M.; Gronenborn, A. M. *J. Magn. Reson.* **1983**, *53*, 423−442.
(26) Landry, S. J.; Gierasch, L. M. *Biochemistry* **1991**, *30*, 7359−7362.
(27) Landy, S. B.; Ray, B. D.; Plateau, P.; Lipkowitz, K. B.; Rao, B. D. N. *Eur. J. Biochem.* **1992**, *205*, 59−69.
(28) Kieffer, B.; Koehl, P.; Plaue, S.; Lefevre, J.-F. *J. Biomol. NMR* **1993**, *3*, 91−112.
(29) Jarori, G. K.; Murali, N.; Rao, B. D. N. *Biochemistry* **1994**, *33*, 6784−6791.
(30) Murali, N.; Jarori, G. K.; Rao, B. D. N. *Biochemistry* **1994**, *33*, 14227−14236.
(31) Andrieux, M.; Leroy, E.; Guittet, E.; Ritco-Vonsovici, M.; Mouratou, B.; Minard, P.; Desmadril, M.; Yon, J. M. *Biochemistry* **1995**, *34*, 842−846.
(32) Koblar, K. S.; Culberson, J. C.; Desolms, S. J.; Giuliani, E. A.; Mosser, S. D.; Omer, C. A.; Pitzenberger, S. M.; Bogusky, M. J. *Protein Sci.* **1995**, *4*, 681−688.
(33) Andersen, N. H.; Nguyen, K. T.; Eaton, H. L. *J. Magn. Reson.* **1985**, *63*, 365−371.

JP952960R